Temporal Image Fractionation: Rejection of Motion Artifacts in Myocardial SPECT

Guido Germano, Paul B. Kavanagh, Hosen Kiat, Kenneth Van Train and Daniel S. Berman

Department of Medical Physics and Imaging, Division of Nuclear Medicine, Department of Imaging and the Division of Cardiology, Department of Medicine, Cedars-Sinai Research Institute, Cedars-Sinai Medical Center, and the Division of Nuclear Medicine and Biophysics, Department of Radiological Sciences and the Department of Medicine, UCLA School of Medicine, Los Angeles, California

Methods: We have developed a protocol, termed "temporal image fractionation," in which static myocardial perfusion SPECT studies are acquired as three-interval dynamic studies (three temporal frames, each consisting of a full projection set), utilizing continuous alternating detector rotation and a multidetector camera. The frames are individually examined for motion by cine display, then summed together into a static SPECT file which is reconstructed with standard procedure. This approach offers three potential advantages in reducing or eliminating image artifacts resulting from patient or organ motion: (1) If severe motion occurs in one frame, only the remaining two are summed and reconstructed (motion-purging); (2) Alternating detector rotation reduces artifacts from mono-directional, drifting motion during acquisition (i.e., upward creep of the heart); and (3) Generally, with multiple rotations, motion is spread over a larger angular range and therefore has a lesser effect on the final reconstructed images. **Results:** These advantages are demonstrated and quantified in this paper using clinical data (A) and simulated motion on phantom data (B and C). In the phantom experiments, fractionated images were found to be 48.9%, 35.8% and 35.9% "more similar" to the original images than nonfractionated images for simulated 1.67-cm upward creep, 1.1-cm nonreturning axial motion and 1.65-cm lateral motion, respectively. **Conclusion:** This protocol requires little extra processing and no final extra data storage compared to standard acquisition, and it has nearly eliminated instances in which a study had to be repeated due to patient motion. Step-and-shoot acquisition is not recommended in conjunction with this protocol, as it would lengthen the time necessary to obtain the same count statistics as in nonfractionated acquisition.

Key Words: myocardial SPECT; dynamic acquisition; fractionation; motion correction

J Nucl Med 1994; 35:1193–1197

Patient or organ motion is perhaps the most common cause of technical inadequacy in myocardial perfusion SPECT, resulting in the need for a repeat study, and, if unrecognized, creating artifacts in the reconstructed images, adversely affecting their visual or quantitative interpretation (*1–3*). Several methods of detection/correction of motion have been reported in the literature, with all the correction algorithms requiring some form of postacquisition processing (*4–10*). Acquisition strategies to reduce motion have essentially consisted of trying to keep the patient still on the bed. In this paper we propose an acquisition approach, termed "temporal image fractionation," which helps eliminate or reduce the effects of motion in myocardial perfusion SPECT.

The introduction of ^{99m}Tc-teboroxime, a myocardial perfusion agent with rapid uptake and washout, has made dynamic myocardial SPECT a reality over the past few years (*11–15*), and modern gamma cameras can support dynamic SPECT acquisition protocols. It is therefore possible to acquire a tomographic study employing several alternating rotations, in other words, to break down a static study into a dynamic study of the same global duration. We call this approach "temporal image fractionation" because it fractionates the total acquisition time into several temporal frames, each frame consisting of a complete set of projection images.

There are several advantages to image fractionation. First, the individual frames can be reviewed side-by-side by displaying their projections in cine mode before reconstruction. This allows elimination of frames in which obvious motion occurred; sum the remainder together and they can be reconstructed into "motion-purged" tomographic images (of course, there is an associated count statistics loss, dependent on the level of fractionation and the number of frames contaminated by motion). Even if the projection images are not reviewed and the frames are simply summed together and reconstructed, image fractionation may still be less sensitive to motion than conventional, static SPECT acquisition protocols. For example, acquiring adjacent frames using alternating detector rotation reduces artifacts from mono-directional, drifting heart motion during acquisition (i.e., upward creep of the heart following exercise) (*16–18*) by averaging such motion at each projection angle. Fractionation of static into dynamic SPECT studies would also alleviate artifacts from the rapid

Received Nov. 29, 1993; revision accepted March 1, 1994.

For correspondence or reprints contact: Guido Germano, PhD, Director, Nuclear Medicine Physics, Cedars-Sinai Medical Center A047 N, 8700 Beverly Blvd., Los Angeles, CA 90048.

variation of a tracer's distribution in the camera's field of view, as reported in pelvic SPECT studies (*19–20*) as well as in ^{99m}Tc-teboroxime myocardial SPECT studies (*21*).

Generally, most types of motion should result in lesser artifacts when image fractionation is used, since motion is "spread" and averaged over a larger angular range than with conventional acquisition. For example, if severe motion of duration T affects T/15 projections out of 60 total projections (or T/5 degrees of the acquisition arc) in a nonfractionated, 180°, 3°/projection, 15 sec/projection acquisition protocol, the same amount of motion would affect n(T/15) projections out of n60 total (or nT/5 degrees of the acquisition arc) in an n-frame, 180°, 3°/projection, 15/n sec/projection fractionated acquisition protocol. The purpose of this paper is to visually and quantitatively demonstrate (A) the advantages of image fractionation + "motion purging" in a clinical study with induced motion, and (B) the motion-rejecting effect of image fractionation in a phantom model with simulated upward creep, lateral motion and axial motion of the heart. We use the specific fractionation protocol routinely employed in our clinic.

METHODS

The image fractionation protocol we investigated called for the acquisition of three frames, each of duration equal to one-third of the conventional "long" or nonfractionated frame (three 5-min frames versus one 15-min frame for clinical ^{99m}Tc-sestamibi or ^{201}Tl, three 1-min frames versus one 3-min frame for ^{99m}Tc phantom experiments). Dynamic (fractionated) SPECT studies were acquired with continuous, alternating CCW and CW rotation and 3° projections using the standard dynamic SPECT acquisition protocol available on our camera. A macro was written to display the projections in the individual frames in cine mode immediately after acquisition; if no major motion is seen in any frame, all frames are automatically summed together projection-by-projection. The entire process adds less than 1 min to processing time. If severe motion is seen in one frame, that frame is discarded and the remaining two are summed (this approach is still valid when the affected frame is the middle one, as long as motion is of the returning type). If two frames (adjacent or not) are contaminated by motion, they are both discarded, and the limitation of the method is the statistical quality of the remaining frame. Once the summed file is generated, processing is resumed as with standard static SPECT studies. The projection data are prefiltered with a two-dimensional Butterworth filter (order = 2.5 and critical frequency = 0.333 cycles/pixel for ^{99m}Tc-sestamibi, order = 5 and critical frequency = 0.25 cycles/pixel for ^{201}Tl, pixel size = 0.53 cm for our acquisitions), reconstructed over 180° (45° RAO to LPO) with a ramp filter and filtered backprojection and reoriented. No attenuation correction was used. A triple-detector camera (Prism 3000, Picker) with LEHR collimators was used for all patient studies and phantom experiments.

Clinical Patients

Over the past 15 mo, more than 1000 patients have had myocardial perfusion ^{99m}Tc-sestamibi and ^{201}Tl SPECT studies performed with the fractionated protocol and the separate dual-isotope technique (*22*). To demonstrate the effect of motion-purging in conjunction with the fractionation protocol, we selected a ^{99m}Tc-sestamibi patient with low likelihood of coronary artery disease, and prompted him to move halfway through the first 5-min acquisition frame. Four 5-min frames were acquired, the last for control purposes. Frames 2 + 3 + 4 (control), as well as Frames 1 + 2 + 3 (fractionated acquisition, nonmotion-purged) and Frames 2 + 3 (fractionated acquisition, motion-purged) were reconstructed and reoriented.

Upward Heart Creep

To test whether image fractionation might reduce artifacts associated with upward heart creep, a chest phantom (Data Spectrum 2230 with cardiac insert 7070) was imaged over three 120-projections, 1-min frames. The phantom's myocardium contained 400 μCi of ^{99m}Tc, and the three frames were also summed together to represent standard or nonfractionated acquisition. Upward creep of 3 pixels (1.65 cm) over the entire study duration was simulated in the standard projection set by shifting projections from 45° to −135° (45° RAO to LPO) by a linearly interpolated distance uniformly varying from 0 to 3 pixels, respectively. In other words, dependence from a multidetector camera was effectively eliminated by considering only projections corresponding to the 180° reconstruction arc, assuming that projections along that arc had been acquired sequentially. In the fractionated sets, projections from 45° to 135° in Frame 1, Frame 2 and Frame 3 were similarly shifted by distances uniformly varying from 0 to 1, 2 to 1 and 2 to 3 pixels, respectively, to account for the alternating detector rotation. Frame 1, Frame 2 and Frame 3 of the fractionated study were summed together and reconstructed simultaneously with the nonfractionated frame, to ensure perfect correlation of the two image datasets. To quantify improvements effected by fractionation, normalized maximal count circumferential profiles were calculated for the unmoved (C_{orig}), moved fractionated (C_{fract}) and moved nonfractionated (C_{nfract}) images. The point-by-point sum of the absolute differences between a pair of 60-point profiles was taken as a measure of their disagreement, which in turn led to the following formula to calculate the percent improvement derived by using fractionation over standard acquisition.

Percent improvement over standard acquisition =

$$\left(1 - \frac{\sum_{i=1}^{60} |[C_i]_{fract} - [C_i]_{orig}|}{\sum_{i=1}^{60} |[C_i]_{nfract} - [C_i]_{orig}|}\right) * 100. \quad \text{Eq. 1}$$

It should be noted that in patient studies the position of the heart with respect to surrounding attenuators is also changing as the heart creeps. Thus, a more rigorous simulation of the upward heart creep phenomenon would keep into account the changing attenuation patterns of the fractionated projection dataset.

Nonreturning Motion

To test whether image fractionation might generally improve reconstructed image quality of studies affected by motion, a nonreturning movement of 2 pixels (1.1 cm) in the y direction (along the patient's axis) at 45 sec from acquisition start was also simulated in the datasets acquired in the previous experiment. Projections from 45° to 0° in the nonfractionated study and projections from 45° to −90° in Frame 1 of the fractionated study were shifted by 2 pixels in y. Again, Frame 1, Frame 2 and Frame 3 of the fractionated study were summed together and reconstructed si-

multaneously with the nonfractionated frame, and Equation 1 was used to quantify the percent improvement derived by using fractionation over standard acquisition. Finally, nonreturning motion of 3 pixels (1.65 cm) in the x direction (perpendicular to the patient's axis) at 45 sec from acquisition start was simulated as described above. Of note, such lateral motion cannot be corrected by standard methods.

RESULTS

In the 100-patient subsample for which records were available, the need for motion-purging (the occurrence of motion in one or more of the fractionated frames) was 14% (28/200), with no significant difference between ^{99m}Tc-sestamibi (15/100) and ^{201}Tl (13/100). The majority of cases involved one frame (25/28 or 89.3%): the first (11/25 or 44%) and the last frame (10/25 or 40%) were most frequently affected, unlike the second frame (4/25 or 16%, two ^{201}Tl and two ^{99m}Tc-sestamibi). This would be expected, as a patient is more likely to move at the beginning of the acquisition (when he/she may still be trying to find a comfortable position), or at the end of the acquisition (when muscle strain sets in, especially if his/her arms are outstretched). A breakdown of the four cases with motion in the middle frame showed motion as likely to be of the nonreturning (2/4, one ^{201}Tl and one ^{99m}Tc-sestamibi) as of the returning type (2/4, one ^{201}Tl and one ^{99m}Tc-sestamibi). In the first instance, Frame 1 and Frame 3 were summed together, in the second the study was repeated (^{201}Tl) or only Frame 1 was used (^{99m}Tc-sestamibi). Motion in two out of the three frames was rare (3/28 or 10.7%). In particular, motion in the first two frames occurred once (^{99m}Tc-sestamibi), motion in the first and third frame twice (one ^{201}Tl and one ^{99m}Tc-sestamibi). Again, while the ^{99m}Tc count statistics allowed the processing of only one frame, the ^{201}Tl study had to be repeated. In conclusion, 26 (92.9%) of the 28 studies affected by motion were salvaged by fractionated acquisition, and only 2 (7.1%) had to be repeated.

Figure 1 shows reconstructed short-axis, midventricular slices of the ^{99m}Tc-sestamibi patient with a low likelihood of coronary artery disease (*23–24*) and induced motion in Frame 1. As expected, cine display of the projections in the fractionated acquisition frames clearly demonstrated severe motion in Frame 1. Summing and processing Frame 2 and Frame 3 only yielded images of good counting statistics and a normal perfusion pattern (center) identical to the pattern shown in the control set (Frames 2 + 3 + 4, left). In contrast, summing and processing Frame 1, Frame 2 and Frame 3 resulted in the artifactual development of a mild anterior and a moderate inferior wall defect in the reconstructed images (right).

Figure 2 shows reconstructed short-axis, midventricular slices of the phantom with simulated upward heart creep. Motion in the projection dataset representing the nonfractionated protocol results in distortion of the left ventricle (LV) shape and development of artifactual defects in the anteroseptal and inferior wall of the reconstructed image

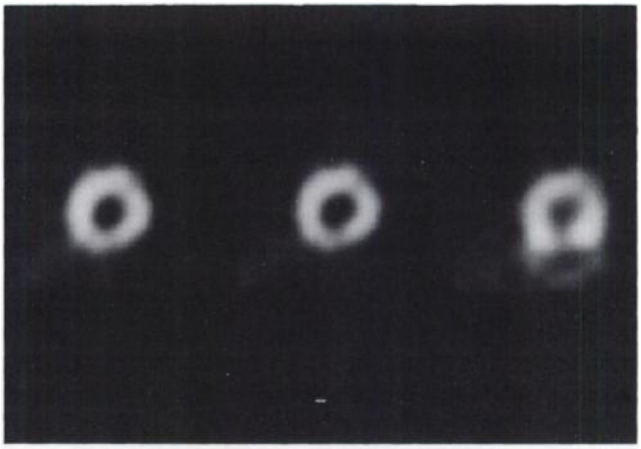

FIGURE 1. Reconstructed short-axis, midventricular slices of a ^{99m}Tc-sestamibi patient with a low likelihood of coronary artery disease and severe motion in Frame 1 of fractionated acquisition. Summing and processing of Frame 2 and Frame 3 yield a normal perfusion pattern (center), identical to that in the control dataset (left). Summing and processing Frame 1, Frame 2 and Frame 3 results in the distortion of the LV shape and the development of an inferior wall defect in the reconstructed image (right).

(right). The same amount of motion with fractionated acquisition does not affect the LV shape and does not change its perfusion pattern (center), resulting in images much more similar to those produced from the original data (left). Figure 3 shows how this similarity was quantified. First, maximal count circumferential profiles were calculated for the images in Figure 2 using appropriate software tools. Then, absolute difference profiles were computed for the original/fractionated and the original/nonfractionated profile pair, and their sums ratioed as in Equation 1. Based on

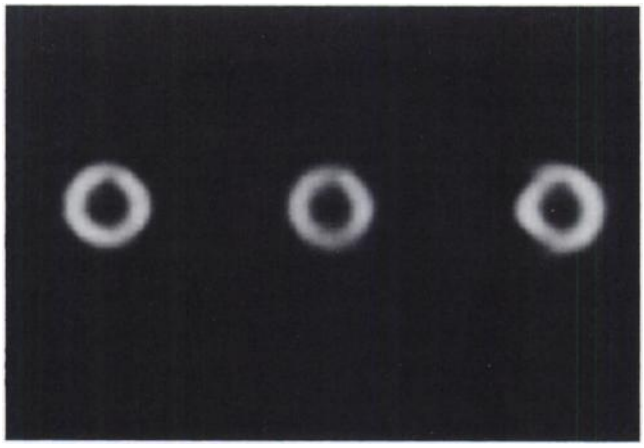

FIGURE 2. Reconstructed short-axis, midventricular slices of the phantom with simulated upward heart creep. The nonfractionated protocol results in distortion of the LV shape and development of artifactual defects in the anteroseptal and inferoseptal wall of the reconstructed image (right). Fractionated acquisition does not affect the LV shape or its perfusion pattern (center), resulting in images more "similar" to those produced from the original data (left), as also demonstrated by the circumferential profiles in Figure 3.

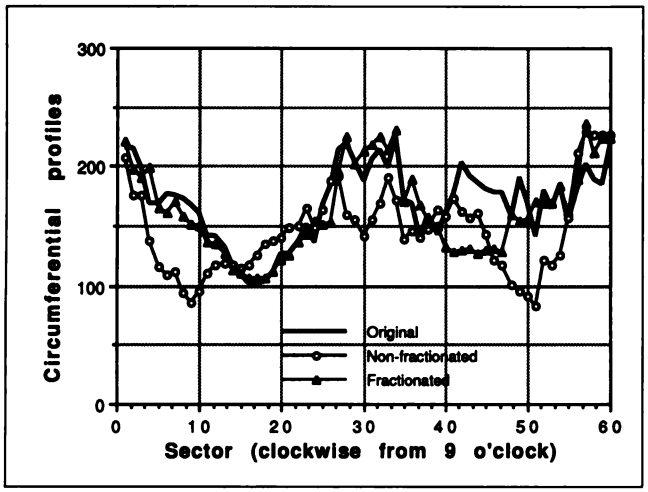

FIGURE 3. Maximal count circumferential profiles for the images in Figure 2. Quantitative analysis of these profiles based on Equation 1 resulted in the fractionated image being judged 48.9% "more similar" to the original than the nonfractionated image.

this criterion, the fractionated image was 48.9% more similar to the original than the nonfractionated image.

Figure 4 shows reconstructed short-axis, midventricular slices of the phantom with simulated nonreturning axial motion. Motion in the projection dataset for the nonfractionated protocol results in distortion of the LV shape and development of an artifactual perfusion defect in the anterior wall of the reconstructed image (right). The same amount of motion with fractionated acquisition does not affect the LV shape nor does it produce defects (center), better matching the normal perfusion pattern of the original data (left). Quantitative maximal circumferential profile analysis based on Equation 1 resulted in the fractionated image being judged 35.8% more similar to the original than the nonfractionated image. Figure 5 shows reconstructed short-axis, midventricular slices of the phantom with simulated nonreturning lateral motion. Motion in the projection dataset for the nonfractionated protocol results in distortion of the LV shape and development of artifactual perfusion defects in the anterior and inferolateral wall of the reconstructed image (right). In contrast, fractionated acquisition does not affect the LV shape nor does it produce defects (center), matching (with only a slight decrease in the wall-to-LV cavity count ratio) the normal perfusion pattern of the original data (left). Quantitative maximal circumferential profile analysis based on Equation 1 resulted in the fractionated image being judged 35.9% more similar to the original than the nonfractionated image.

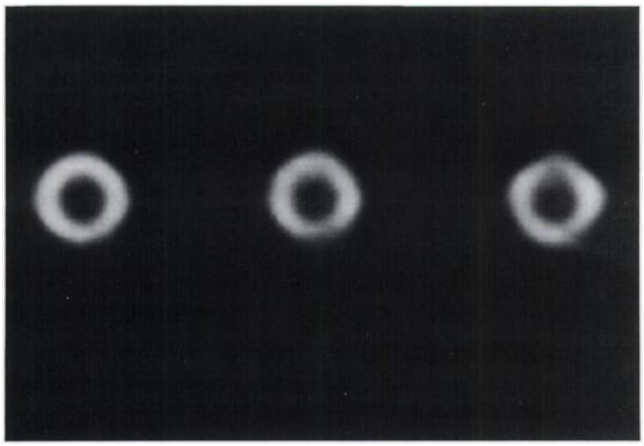

FIGURE 4. Reconstructed short-axis, midventricular slices of the phantom with simulated nonreturning axial motion. The nonfractionated protocol results in distortion of the LV shape and development of an artifactual defect in the anterior and inferolateral wall of the reconstructed image (right). Fractionated acquisition does not affect the LV shape nor does it produce defects (center), matching the normal perfusion pattern of the original data (left). Quantitative analysis of the maximal count circumferential profiles based on Equation 1 resulted in the fractionated image being judged 35.8% "more similar" to the original than the nonfractionated image.

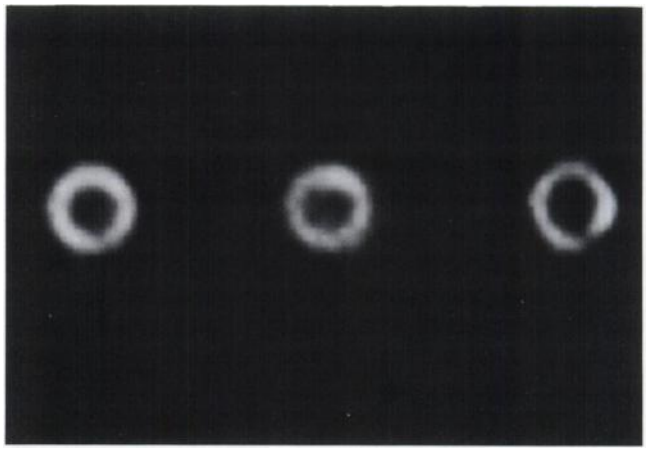

FIGURE 5. Reconstructed short-axis, midventricular slices of the phantom with simulated nonreturning lateral motion. The nonfractionated protocol results in distortion of the LV shape and development of artifactual defects in the anterior and inferolateral wall of the reconstructed image (right). Fractionated acquisition does not affect the LV shape nor does it produce defects (center), matching the normal perfusion pattern of the original data (left). Quantitative analysis of the maximal count circumferential profiles based on Equation 1 resulted in the fractionated image being judged 35.9% "more similar" to the original than the nonfractionated image.

DISCUSSION

In this paper, we have presented a new acquisition/processing protocol to reduce or eliminate artifacts and inaccuracies derived from patient or organ motion in myocardial SPECT studies. The technique uses (but does not necessarily require) a multidetector camera in conjunction with continuous, alternating rotation to fractionate the acquisition frame into three sub-frames, and proved visually and quantitatively effective in correcting motion-corrupted clinical and phantom data. The appeal of this technique lies in the fact that improvements in image quality and artifact reduction are achieved with little or no extra processing, and ultimately no additional data storage requirements. Fractionation of static into dynamic SPECT studies also minimizes artifacts from the rapid variation of a tracer's

distribution during acquisition (*19–20*), and is by no means limited to myocardial applications. In fact, it is applicable to all organs (e.g., brain SPECT, bone SPECT, gallium SPECT, and even static non-SPECT imaging) which require long acquisitions.

It should be noted that if motion is substantial, images reconstructed from fractionated projection data may still contain artifactual defects. Such is the case in Figure 1 (right), where motion in Frame 1 is so severe as to cause an artifactual inferior wall defect even when fractionation is used. Thus, we recommend cine review of the projection data and (if needed) motion-purging in all patients studied with the fractionated protocol. In cases where motion is found not to be confined to one frame, or is of the non-returning type and occurs in the middle frame, our experience shows that it is possible to obtain adequate data for interpretation from one frame only (5 min) in ^{99m}Tc-sestamibi studies, an option not available with regular acquisition. However, 5-min ^{201}Tl images usually suffer from low count statistics. In these instances it is better to repeat the ^{201}Tl acquisition, although possible alternatives include acquiring a fourth 5-min frame, using a smoother prereconstruction filter or applying a more conventional motion correction algorithm to the data (*4–10*). Finally, although not indispensable, continuous or pseudo-continuous (modified step-and-shoot) acquisition is highly desirable with fractionation (*25*). Assuming a "dead time" (time necessary to step between adjacent projections) of 5 sec/projection for a single-detector camera operated in the step-and-shoot, 180°, 3° per projection acquisition mode (15 sec/projection for a standard nonfractionated clinical acquisition), fractionation would cause a 50% increase in study time, from 20 to 30 min.

Additional work will be needed to establish optimal fractionation protocols. Also, conclusive evidence as to whether fractionation without motion-purging is preferable to standard acquisition would require a more extensive investigation of motion patterns and myocardial activity distributions than attempted in this paper. Similarly, the use of fractionation in combination with other acquisition, pre-processing and analysis techniques should be carefully investigated. We have not performed a quantitative or qualitative assessment of the changes in sensitivity and specificity for ^{99m}Tc-sestamibi or ^{201}Tl myocardial SPECT studies following the application of our fractionated acquisition protocol. Future extensions of this work should include validation of the technique in a prospective patient population using quantitative analysis to clearly assess the clinical significance of this novel motion rejection approach.

REFERENCES

1. Botvinick E, Zhu Y, O'Connell W, Dae M. A quantitative assessment of patient motion and its effect on myocardial perfusion SPECT images. *J Nucl Med* 1993;34:303–310.
2. Cooper J, Neumann P, McCandless B. Effect of patient motion on tomographic myocardial perfusion imaging. *J Nucl Med* 1992;33:1566–1571.
3. Eisner R. Sensitivity of SPECT thallium-201 myocardial perfusion imaging to patient motion. *J Nucl Med* 1992;33(8):1571–1573.
4. Cooper J, Neumann P, McCandless B. Detection of patient motion during tomographic myocardial perfusion imaging. *J Nucl Med* 1993; 34:1341–1348.
5. De Agostini A, Moretti R, Belletti S, et al. A motion correction algorithm for an image realignment programme useful for sequential radionuclide renography. *Eur J Nucl Med* 1992;19:476–483.
6. Eisner R, Noever T, Nowak D, et al. Use of cross-correlation function to detect patient motion during SPECT imaging. *J Nucl Med* 1987; 28:97–101.
7. Friedman J, Berman D, Van Train K, et al. Patient motion in thallium-201 myocardial SPECT imaging: an easily identified frequent source of artifactual defect. *J Nucl Med* 1988;13:321–324.
8. Germano G, Chua T, Kavanagh P, Kiat H, Berman D. Detection and correction of patient motion in dynamic and static myocardial SPECT using a multi-detector camera. *J Nucl Med* 1993;34:1349–1355.
9. Parker A. Effect of motion on cardiac SPECT imaging [Editorial]. *J Nucl Med* 1993;34:1355–1356.
10. Yang C, Orphanoudakis S, Strohbehn J, et al. A simulation study of motion artifacts in computed tomography. *Phys Med Biol* 1982;27:51–61.
11. Berman D, Kiat H, Maddahi J. The new ^{99m}Tc myocardial perfusion imaging agents: ^{99m}Tc-sestamibi and ^{99m}Tc-teboroxime. *Circulation* 1991; 84:I7–I21.
12. Leppo J, DePuey E, Johnson L. A review of cardiac imaging with sestamibi and teboroxime. *J Nucl Med* 1991;32:2012–2022.
13. Li Q, Solot G, Frank T, Wagner H, Becker L. Tomographic myocardial perfusion imaging with technetium-99m-teboroxime at rest and after dypiridamole. *J Nucl Med* 1991;32:1968–1976.
14. Stewart R, Heyl B, O'Rourke R, Blumhardt R, Miller D. Demonstration of differential post-stenotic myocardial technetium-99m-teboroxime clearance kinetics after experimental ischemia and hyperemic stress. *J Nucl Med* 1991;32:2000–2008.
15. Nakajima K, Taki J, Bunko H, et al. Dynamic acquisition with a three-headed SPECT system: application to technetium-99m-SQ30217 myocardial imaging. *J Nucl Med* 1991;32:1273–1277.
16. Friedman J, Van Train K, Maddahi J, et al. "Upward creep" of the heart: a frequent source of false-positive reversible defects during thallium-201 stress-redistribution SPECT. *J Nucl Med* 1989;30:1718–1722.
17. Mester J, Weller R, Clausen M, et al. Upward creep of the heart in exercise thallium 201 single photon emission tomography: clinical relevance and a simple correction method. *Eur J Nucl Med* 1991;18:184–190.
18. He Z, Darcourt J, Benoliel J, et al. Major upward creep of the heart during exercise thallium-201 myocardial SPECT in a patient with chronic obstructive pulmonary disease. *J Nucl Med* 1992;33:1846–1847.
19. Bok B, Bice A, Clausen M, Wong D, Wahner H. Artifacts in camera based single photon emission tomography due to time activity variation. *Eur J Nucl Med* 1987;13:439–442.
20. O'Connor M, Kelly B. Evaluation of techniques for the elimination of "hot" bladder artifacts in SPECT of the pelvis. *J Nucl Med* 1990; 31:1872–1875.
21. O'Connor M, Cho D. Rapid radiotracer washout from the heart: effect on image quality in SPECT performed with a single-headed gamma camera system. *J Nucl Med* 1992;33:1146–1151.
22. Berman D, Kiat H, Friedman J, et al. Separate acquisition rest thallium-201/stress technetium-99m sestamibi dual isotope myocardial perfusion SPECT: a clinical validation study. *J Am Coll Cardiol* 1993;22:1455–1464.
23. Rozanski A, Diamond G, Berman D, et al. The declining specificity of exercise radionuclide ventriculography. *N Engl J Med* 1983;309:518–522.
24. Rozanski A, Diamond G, Forrester J, et al. Alternative referent standards for cardiac normality. Implications for diagnostic testing. *Ann Intern Med* 1984;101:164–171.
25. Germano G, Van Train K, Garcia E, et al. Quantitation of myocardial perfusion with SPECT: current issues and future trends. In: Zaret B, Beller G, eds. *Nuclear cardiology: the state of the art and future directions*. St Louis: Mosby Year Book; 1992:77–88.